Vol. 1 / Issue 2 / 2024

FEZ MULTIDISCIPLINARY JOURNALS

Journal of Biology and Biomedical Research

ISSN: 3009-5522

Journal homepage: https://fmjpublishing.com/index.php/J2BR

Research article

HPLC analysis, hemolytic activity, and acute toxicity of *Haplophyllum tuberculatum* (Forssk.) aqueous extract and in silico study

Abdelkrim Agour[a,*], Najoua Soulo[a], Mohammed Bassouya[b], Mohamed Amine El Hajjaji[a], Amina Bari[b], Elhoussine Derwich [a]

a Laboratory of Biotechnology, Conservation and Valorization of Bioressources, Faculty of Sciences Dhar El Mahraz, University Sidi Mohamed Ben Abdellah, Fez30050, Morocco

b Laboratory of Biotechnology, Environment, Agrifood, and Health, Faculty of Sciences Dhar El Mahraz, University of Sidi Mohamed Ben Abdellah, Fez 30050, Morocco

*Corresponding author: Abdelkrim Agour (Abdelkrim.agour@usmba.ac.ma)

Abstract

Plant-derived compounds are increasingly explored as alternatives to synthetic drugs, which, despite their efficacy, may induce adverse effects such as hepatotoxicity and nephrotoxicity. This study aims to characterize the phytochemical profile of *Haplophyllum tuberculatum* (Forssk.) aqueous extract (HTAE) using HPLC-DAD and colorimetric assays, assess its acute toxicity, evaluate its hemolytic activity on rat red blood cells (RBCs), and perform molecular docking to predict interactions with hemoglobin. HTAE, obtained by infusing the powdered aerial parts in boiling water, yielded 15.08%. Colorimetric assays indicated a high total polyphenol content (41.18±1.99 mg GAE/g extract), a notable concentration of condensed tannins (7.09 ± 0.27 mg TAE/g extract), and a lower flavonoid content (4.33±0.45 mg QE/g extract). HPLC-DAD analysis identified gallic acid, caffeic acid, and rosmarinic acid as principal phenolic constituents. Acute toxicity was assessed in rats at doses of 1000 mg/kg and 2000 mg/kg over 14 days, with no significant changes in body weight, relative organ weights, or biochemical markers (ALAT, ASAT, urea, and creatinine), suggesting an LD_{50} > 2000 mg/kg. Molecular docking analysis demonstrated that rosmarinic and gallic acids exhibited notable binding affinities to human hemoglobin (-5.503 and -5.154 kcal/mol, respectively). HTAE induced only a weak hemolytic effect on RBCs. These findings highlight the potential safety of HTAE at tested doses and suggest its possible use in pharmacological applications while minimizing synthetic drug-associated toxicity.

Keywords: Hemolytic; Acute toxicity; *H. tuberculatum*; HPLC-DAD; Polyphenols

Citation: Agour, A.; Soulo, N.; Bassouya, M.; El Hajjaji, M.A; Bari, A.; Derwich, E. HPLC analysis, hemolytic activity and acute toxicity of *Haplophyllum tuberculatum* (Forssk.) aqueous extract and in silico study. *Journal of Biology and Biomedical Research*. 2024,1(2), 117-127. https://doi.org/10.69998/j2br.v1i2.19

Edited by: Ibrahim Mssillou

1. Introduction

Herbal medicine relies on medicinal plants as valuable sources of therapeutic agents, many of which belong to diverse botanical families and are widely used in traditional medical practices (Mssillou et al., 2021; Amrati et al., 2023a). The Rutaceae family, which includes 2,100 species, is one of the main botanical families used by people around the world for traditional medicine (Junior et al., 2023). One of these species is *Haplophyllum tuberculatum* Forssk. (*H. tuberculatum*), known for its wide-ranging traditional uses, including antiseptic, vermifuge, calming, hypnotic, treatment for ulcers, diabetes, abdominal bloating, ear infections, fever, liver diseases, rheumatism, diarrhea, obesity, constipation, hypertension, colon diseases, menstrual pain, and heart diseases (Hadjadj et al., 2015). Bioactive compounds derived from plants are increasingly explored as alternatives to synthetic pharmaceuticals. While these drugs exhibit precise pharmacological targets, they may also induce cytotoxic effects, potentially leading to hepatotoxicity and nephrotoxicity (Wu and Chen, 2022).

Extracts from *H. tuberculatum* have already been extensively studied for their biological activities, which raises concerns about the novelty of the present investigation. Used for its antiprotozoal properties, we find that the aqueous and chloroform fractions derived from partitioning an ethanolic extract of the *H.* tuberculatum roots exhibited antiprotozoal activity against *Plasmodium falciparum* and *Leishmania donovani,* displaying over 85% inhibition of growth at 10 µg/mL (Mahmoud et al., 2020b). The lignans from *H. tuberculatum*, particularly Nectandrin B, exhibited significant activity against axenic amastigotes

Received: November 05, 2024; **Revised:** January 30, 2025; **Accepted:** April 14, 2025; **Published:** May 10, 2025

of *Leishmania donovani* (IC_{50} = 4.5 µM), while the lignan 3,30-dimethoxy-4,40-dihydroxylignan-9-ol demonstrated high activity against *Plasmodium falciparum* (IC_{50} = 9.3 µM) (Mahmoud et al., 2020a).

Botanical extracts of *H. tuberculatum* are also characterized by their antimicrobial activity. Moreover, fractions (methanolic, hexanic, chloroformic, ethyl acetate, butanolic, and aqueous) prepared from the aerial parts of *H. tuberculatum* exert activity against both Gram-positive and Gram-negative bacterial strains (Al-Saeghi et al., 2022). Furthermore, the ethanol whole-plant extract, at concentrations of 1%, 2%, and 3%, suppressed fungal isolates *Fusarium culmorum* and *Rhizoctonia solani* (Abdelkhalek et al., 2020). Lastly, treatment of *Chenopodium amaranticolor* with an ethanolic extract of *H. tuberculatum* significantly inhibits their infection by tobacco mosaic virus (Abdelkhalek et al., 2020).

Previous studies have reported anticancer activity of compounds extracted from *H. tuberculatum*. Sabry et al. (Mohamed Mohamed Sabry et al., 2016) reported that the essential oil extracted from the aerial parts of *H. tuberculatum* demonstrates potential activity against carcinoma cell lines of the lung (H-1299) and liver (HEPG2) with 4.7µg/ml and 4.1 µg/ml, respectively. While Al-Nour et al. 2021 reported that the *H. tuberculatum* aerial parts ethanol extract shows anticancer potential, phytochemicals including polygamain, justicidin A, justicidin B, γ-fagarine, skimmianine, haplotubine, kusunokinin, and flindersine contribute to its cytotoxicity by targeting key processes like cell growth, proliferation, survival, apoptosis induction, metastasis, and drug resistance. In another study, the chloroform extract of *H. tuberculatum* exhibits cytotoxicity against melanoma cells (GI_{50} = 0.45 µg/mL), with its cytotoxic effect correlated with cell cycle arrest in the S phase and a high percentage of cells showing reduced DNA content in A375 cells (AlQathama et al., 2022). In fact, the aerial parts extract of *H. tuberculatum* exhibited cytotoxic activity against the RAMOS cell line with an IC_{50} value of 25.3 µg/mL, against the U937 cell line with an IC_{50} value of 29.3 µg/mL, and against the RPMI-8866 cell line with an IC_{50} value of 31.8 µg/mL among hematopoietic tumor cell lines (Varamini et al., 2007).

The aqueous extract of *H. tuberculatum* (HTAE) is commonly used in the treatment of various ailments; however, data regarding its toxicity remain limited. Furthermore, evaluating the cytotoxicity of HTAE is essential, particularly in the context of potential oral or injectable administration. The aim of this study is to determine the chemical composition of HTAE by HPLC-DAD, assess its acute toxicity, evaluate its hemolytic activity on rat red blood cells (RBC), and performs *in silico* study.

2. Materials and methods

2.1. Plant material

In February 2021, flowering aerial parts of H. tuberculatum (Figure 1) were collected in south-eastern Morocco, near the town of Akka (29°22.5"N 8°16"W). The scientific name of the species studied was determined at the Biotechnology, Environment, Agri-food, and Health Laboratory of the Dhar El Mahraz Faculty of Sciences, USMBA, Fez. A specimen has been deposited in the herbarium of the same laboratory under number HT0019220211.

Figure 1. *H. tuberculatum* in the flowering stage

2.2. Preparation of H. tuberculatum aqueous extract

HTAE was prepared using the infusion method. The *H. tuberculatum* plant material was air-dried and then ground using a Waring® blender. 70 g of the powder obtained was added to 700 ml of boiling water. After 20 minutes, the mixture was filtered through Whatman No. 1 paper. The filtrate was then dried at 37°C (Agour et al., 2022a).

2.3. HPLC-DAD analysis

Preparation of standards: The standard molecules in this analysis are gallic acid, caffeic acid, vanillin, rutin, quercetin, catechin, rosmarinic acid, luteolin, arbutin, and ferulic acid (Sigma-Aldrich, Germany). The standards are prepared in methanol at 100 ppm.

Operating conditions: A Shimadzu HPLC-system with an analytical column (C18) SGE 250x4.6mm SS Exsil ODS 5 µm was used. A gradient separation was performed using two solvents (M (H2O/acetic acid) (97.5: 2.5, v/v) and N (MetOH/acetonitrile) (50: 50, v/v)). The injection volume was 20 µL, and the flow rate was 1 mL/minute. Detection was carried out with wavelengths varying between 200 and 800 nm. The elution gradient was at 0 min (5% X, 95% Y), 6.25 min (30% M, 70% N), 12.5 min (35% M, 65% N), 16.25 min (70% M, 30% N), 17.5 min (100% M, 0% N), and 18.75 min (5% M, 95% N) (Mssillou et al., 2022).

2.4. Total polyphenols, flavonoids, and condensed tannins

2.4.1. Determination of total polyphenol content (TPC)

A volume of 400 µL of diluted Folin reagent (1/10) will be added to 80 µL of diluted sample. After 4 minutes, 320 µL of sodium carbonate (75 mg/mL) will be added to the previous mixture. The mixture will then be incubated for 2 hours at room temperature in the laboratory. The optical density will be measured at 760 nm. The Total Phenolic Content (TPC) will be expressed in mg of gallic acid equivalents per gram of extract (mg GAE/g Ext), utilizing a gallic acid calibration range (equation: y = 5.392x + 0.012; R^2 = 0.993) (Boizot et al., 2020).

2.4.2. Determination of total Flavonoid (Fl)

The flavonoids present in HTAE were quantified using the method previously described in the literature with slight modifications (Bahorun et al., 1996). A volume of 1.25 mL of diluted extract was added to 1.25 mL of AlCl3 (2%). After an incubation period (30 min) at laboratory

temperature in the dark, we measured the optical density at 430 nm Fl in HTAE, expressed as milligrams of Quercetin equivalent per g of extract (mg QE/g Ext) using a calibration curve (Y=13.998x+0.113; R^2 = 0.99).

2.4.3. Determination of condensed tannins (CT)

TC concentrations in HTAE were determined using a method previously described in the literature with some modifications (Joslyn, 1970). 300 µL of each dilution of HTAE were mixed with 900 µL of Folin-Ciocalteu and 3 mL of sodium carbonate (7.5%). Absorbance was measured at 760 nm after incubation for 30 min in the dark at laboratory temperature. TC concentrations in HTAE are expressed as milligrams of tannic acid equivalent (TAE) per gram of extract (mg TAE/g Ext): y = 5.615x - 0.0005 (R^2 = 0.9871).

2.5. Acute toxicity test

The acute toxicity of *C. cinerea* extracts was assessed in accordance with OECD guideline N° 423. CCA and CCE were tested at two distinct doses (1000 and 2000 mg/kg) on fasted mice for 12 hours. Five groups of animals (males and females) were used (n = 7). Extracts were administered orally by gastric gavage for each group. The negative control group received 0.9% NaCl.

2.5.1. Handling and housing of animals

To perform the acute toxicity test, male and female mice (0.03-0.04 kg) were obtained from the Department of Biology, Faculty of Sciences Dhar El-Mahraz, Sidi Mohamed Ben Abdellah University, Fez, Morocco. Animal housing conditions were as follows: Temperature (28-32 °C); humidity (50-55%); day/night photoperiod (~12/12 h). Mice used in this test had free access to food and were handled with the approval of the ethics committee (LBEAS-February 2021).

2.5.2. Body weight measurement and signs of toxicity

Groups of mice were observed prior to oral administration of HTAE and then examined every hour for five hours, then at 24 hours, and finally every day for 14 days. Body weight measurements were taken every 3 days**.** All observations were meticulously documented, maintaining individualized records for each animal. Cage assessments encompass evaluation of skin and fur conditions, ocular health, respiratory parameters, autonomic responses (salivation, diarrhea, and urination), central nervous system manifestations (tremors, convulsions, tail curling, ptosis, relaxation, behavioral alterations, gait and posture variations, response to handling), changes in strength, and stereotypical behaviors (Demma et al., 2007),(Nair et al., 2009).

2.5.3. Relative organ weights (ROW)

At the end of the 14-day acute toxicity period, the relative kidney and liver weights of each mouse are calculated according to Kifayatullah et al. 2015 as follows:

$$\boldsymbol{ROW = \frac{Organ\ weight(g)}{Animal\ body\ weight(g)} \times 100}$$

ROW: Relative organ weights

2.5.4. Analysis of biochemical parameters

After anesthetizing the mice with sodium pentobarbital intraperitoneally at a dose of 30 mg/kg and sacrificing them, blood samples were taken by cardiac puncture into heparinized tubes, then centrifuged at 1500 rpm for 10 min. Animal sera were recovered for analysis of the following biochemical parameters: creatinine, urea, aspartate aminotransferase (ASAT), and alanine aminotransferase (ALAT) (Ramadan et al., 2012).

2.6. Red Blood Cell Preparation

Freshly obtained rat blood samples were combined with a heparin anticoagulant solution. To obtain a purified erythrocyte suspension, the blood sample underwent three successive washes with sterile NaCl saline (0.9%). After each wash, the cells were separated by centrifugation (3500 rpm for 10 minutes at 4°C) and the supernatant was carefully aspirated. Finally, the erythrocytes were reconstituted in saline to form a 3% solution for use in the hemolytic assay.

2.7. Hemolytic Assay

The evaluation of the hemolytic activity of the investigated plant was conducted following the modified protocol previously described (Saleh et al., 2021). In hemolysis tubes, 50 µL of various initial concentrations of the extract (5, 25, 50, and 100 mg/mL) was combined with 1950 µL of the prepared erythrocyte suspension. The mixtures obtained were then incubated at 37 °C for one hour in a water bath. At 15-minute intervals over 60 minutes, 500 µL from each tube was extracted and mixed with 1.5 mL of a phosphate buffered saline (PBS) solution. Following this, the tubes underwent centrifugation at 3000 rpm for 10 minutes. Finally, the absorbance of supernatants was measured at 540 nm (representing hemoglobin absorbance after erythrocyte lysis) using a UV-visible spectrophotometer against a blank containing PBS. A negative control tube was prepared under identical experimental conditions, comprising 500 µL of erythrocyte suspension and 1500 µL of PBS buffer, without extract.

The percentage of hemolysis was determined relative to a total hemolysis tube, containing 500 µL of erythrocyte suspension and 2500 µL of distilled water under similar conditions. The hemolysis rate for the extract samples was calculated as a percentage (%) of total hemolysis after 60 minutes of incubation, using the following equation:

$$\textbf{Hemolysis rate (\%)} = [(A - A_0) / (A_t - A_0)] \times 100$$

A, A_0, and A_t were the absorbance of the sample, the absorbance of the negative control, and the absorbance of the positive control (total hemolysis), respectively.

2.8. In silico study

2.8.1. Ligand preparation

The chemical constituents of the aqueous extract of *H. tuberculatum* determined by HPLC-DAD analysis were obtained from the PubChem database in .SDF format. To prepare the docking ligands, we used the OPLS3 force field implemented in the Maestro LigPrep module developed by Schrödinger. Each initial input structure was transformed into up to 32 different structural forms, containing variations in stereochemistry, ionization, and tautomeric configurations. These structures were then subjected to treatments including energy minimization and geometry optimization. Adjustments of ionization and tautomeric states were performed using the Epik tool at a physiological pH of 7.0 ± 2.0 (Ouahabi et al., 2023).

2.8.2. Receptor preparation

The crystal structures of the human TRPV4 ankyrin repeat domain (PDB: 4DX1) (Zhou et al., 2020), the anion exchanger domain of human erythrocyte Band 3 (PDB ID:

4YZF) (Fofana et al., n.d.), and human hemoglobin in the deoxy form (PDB ID: 2DN2) (Tellone et al., 2012) were obtained from the Protein Data Bank. In the Maestro software, Schrödinger used the Protein Preparation Wizard to ensure the chemical accuracy and optimization of these proteins to make them suitable for model calculations. At this stage, several measures were taken, including the assignment of bond orders, the introduction of hydrogen atoms in the structure, the formation of disulfide bonds, the adjustment of zero-order bonds on the metal, and the removal of water molecules more than 5 Å from heteroatoms (Lafraxo et al., 2022).

The pH 7, ionization predictions and tautomeric states were performed for the heteroatom groups in the appropriate configuration. Prime was used to fill in the missing side chains in the protein crystal structures. To simulate a pH of 7.0, which accommodates ionization states suitable for both acidic and basic amino acid residues, hydrogen bonds were added. It should be noted that the introduction of hydrogen atoms occasionally resulted in steric clashes among the residues. These clashes were resolved through energy minimization, employing the OPLS3 force field, until an RMSD value of 0.30 Å was achieved (El Abdali et al., 2023).

2.8.3. Receptor Grid Generation

The investigation and characterization of the active site (binding pockets) within the proteins were carried out using the receptor grid generation wizard of the maestro software selected on an atom in the original ligand (an option offered by receptor grid generation wizard). The only active site generated and used for the subsequent grid creation.

2.8.4. Molecular docking

The evaluation of ligand values was performed using the Glide module of the Schrodinger software using default settings in standard precision (SP) mode as described in the references provided. During this process, Glide uses a series of stepwise filters to examine the possible binding orientations of the ligand in the receptor active site. The ligand is treated as a tunable entity, while the receptor remains rigid except for the active site region. The docking score is then calculated and the ligands are ranked according to their Gscore (SP) (Bouslamti et al., 2022).

2.9. Statistical analysis

The tests conducted in this research were triplicated and expressed by mean ± standard deviation. GraphPad Prism software (version 5) was used to perform the analysis using one-way analysis of variance (ANOVA) followed by Tuckey-test. Differences at $P < 0.05$ were considered significant.

3. Results and discussion

3.1. Colorimetric assays

The yield obtained by infusing the powdered aerial parts of *H. tuberculatum* in boiling water is 15.08%. Colorimetric assays revealed that HTAE contains a very high amount of TPC (41.18±1.99 mg GAE/g Ext), a remarkable amount of CT (7.09±0.27 mg TAE/g Ext), and a low content of Fl (4.33±0.45 QE/g Ext). These results agree with some results reported in the bibliography and differ from others. Eissa et al., (2013) reported that the hydroethanolic extract of *H. tuberculatum* had a polyphenol content on the order of 46.2 mg EAG/g ext. The work of Djouahra Fahem et al. (2023) showed that the TPC in *H. tuberculatum* is estimated to be 74.45 mg EAG/g of dry matter in polyphenolic extract. *H. tuberculatum* extracts show variations in their total polyphenol content depending on the polarity of the solvents used and the effects of various factors, such as the regions and seasons in which the plant is collected, the part studied (leaves vs. aerial parts), and the extraction process (Agour et al., 2022a). In contrast, the study by Hamdi et al. (Hamdi et al., 2018b) showed that ethyl acetate and n-butanol extracts of *H. tuberculatum* exhibited high levels of PTC, with values of 262 and 256 mg GAE/mg, respectively. Ethyl acetate had the highest flavonoid content (99.1 mg EQ/g of dry weight), while the n-butanol extract had a tannin content of 1115 mg catechin/g of dry weight.

3.2. HPLC-DAD analysis of HTAE

Qualitative analysis of *H. tuberculatum* aqueous extract by HPLC-DAD revealed the presence of mainly phenolic acids: gallic acid (1), caffeic acid (2), and rosmarinic acid (3) (Figure 2). These findings complement previous quantitative chromatographic analyses of HTAE (the same extract) by LC-MS (Agour et al., 2022a), and this technique revealed the richness of HTAE in Kaempferol-3-O-hexose deoxyhexose (49.08%), Proanthocyanidin (18.75%), Kaempferol-3-O-glucose (6.37%), Quercetin-3-O-hexose deoxyhexose (6.24%), Quercetin-3-O-glucuronic acid (4.18%), Kaempferol-3-O-glucuronic acid (2.90%), and Protocatechic acid (0.19%).

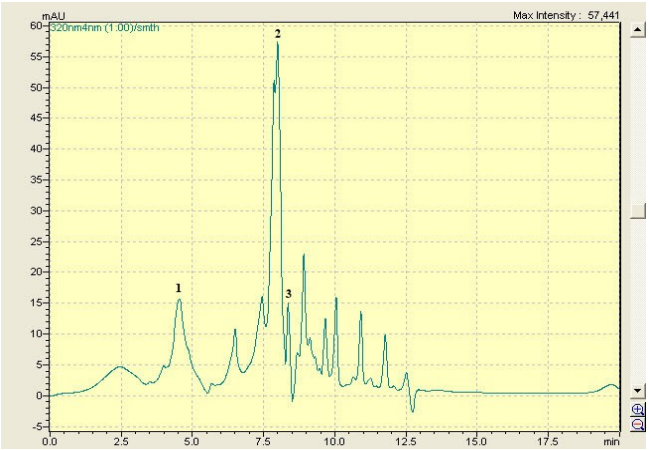

A- Chromatogram obtained by HPLC-DAD analysis of HTAE

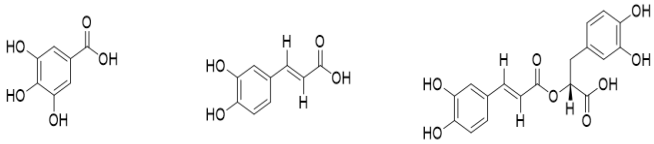

Gallic acid (1) Caffeic acid (2) Rosmarinic acid (3)

B- molecule structures identified by HPLC-DAD

Figure 2. Compounds identified in aqueous extract of *Haplophyllum tuberculatum*

Table 1. Phenolic compounds identified in HTAE

Phenolic Compounds	Formula	RT (min)	UV (nm)
Gallic acid	$C_7H_6O_5$	4.69	280
Caffeic acid	$C_9H_8O_4$	7.77	300
Rosmarinic acid	$C_{18}H_{16}O_8$	8.30	320

H. tuberculatum is known for its phytochemical composition rich in bioactive compounds such as phenolics, alkaloids, and saponins. The variation in compounds identified from *H. tuberculatum* mainly varies according to the plant material used, extraction solvents, and analytical techniques (Arabsalehi et al., 2022; Mirniyam et al., 2022; Gharibi et al., 2019). However, Hosseini et al. (2021) reported that dichloromethane, methanol, chloroform, n-hexane, ethyl acetate, and petroleum ether can be effective in extracting compounds such as alkaloids, lignans, and coumarins, while ethanol was very useful for extracting different classes of polar and non-polar compounds. Among the phenolic compounds reported in *H. tuberculatum* extracts are flavonoids, coumarins, and lignans. Ammoidin, detected by HPLC-UV, is a coumarin isolated from a petroleum ether extract (Khalid et Waterman , 1981). 5,7,4'-Trihydroxy-6-methoxy-3-O-glucosyl flavone is identified in an ethyl acetate extract of *H. tuberculatum* (Kalid et Waterman, 1981). *H. tuberculatum* also contains fatty acids, as chromatographic analysis revealed that the petroleum ether extract of this species contains γ-linolenic acid, linoleic acid, and palmitic acid (Hamdi et al., 2018a). Eissa et al. (Eissa et al., 2013) reported that the HPLC-MS method revealed the presence of methoxyflavones, flavonols, cinnamic acids, and benzoic acids as the main chemical constituents. Abdelkhalek et al. (2020) reported that the analysis of the *H. tuberculatum* ethanol whole plant extract by HPLC revealed that this extract contained resveratrol (5178.58 mg/kg), kaempferol (1735.23 mg/kg), myricetin (561.18 mg/kg), rutin (487.04 mg/kg), quercetin (401.04 mg/kg), and rosmarinic acid (387.33 mg/kg).

3.3. Acute toxicity

3.3.1. Evolution of animal body weight over 15 days

The results of changes in animal body weight over the acute toxicity test period are shown in Figure 3. On day 0, the body weights of animals in the various groups were 31.32 ± 1.90 g, 30.41 ± 1.51 g, and 28.95 ± 2.54 g for the 1000 mg/kg, 2000 mg/kg, and negative control groups, respectively. From the start of the trial, all groups showed a normal increase in body weight, but after day 9, weight continued to increase in the 1000 mg/kg and negative control groups, with mean values for day 15 of 36.98 ± 3.16 g and 35.88 ± 3.11 g, respectively. In contrast, between days 9 and 15, the 2000 mg/kg group showed a slight decrease in mean body weight (33.09 ± 1.88 g on day 15 post-treatment). Statistically, the differences observed between the groups were not significant. Thus, the aqueous extract of *H. tuberculatum* had no effect on the body weight of mice used in this acute toxicity test.

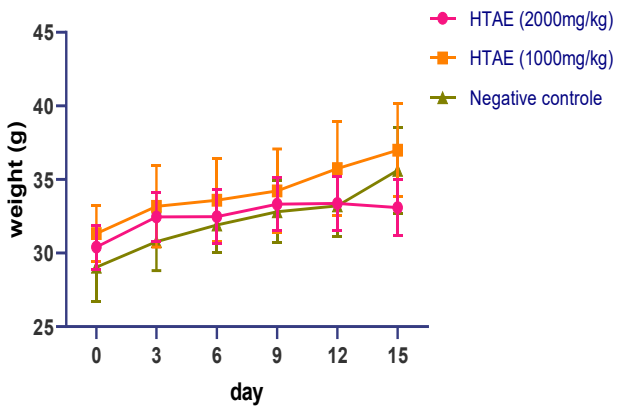

Figure 3. Variation in animal body weight over 15 days

3.3.2. Relative liver and kidney weights 15 days after treatment

The results presented in Figure 4 show the relative liver and kidney weights of the mice. These results demonstrate that the mean relative liver weight was 4.24±0.34% and 4.21±1.08% for the HTAE (2000 mg/ml) and negative control groups, respectively. The relative kidney weight was 1.36±0.13% for the treated group, with no significant difference from the negative control group.

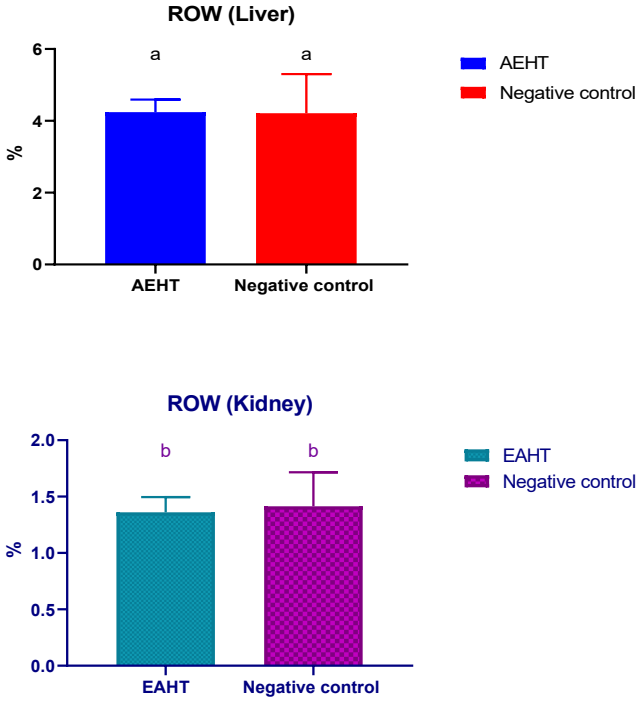

Figure 4. Relative liver and kidney weights 15 days after treatment with HTAE**.** For each parameter, bars with different letters represent statistically different values ($p < 0.05$)

3.3.3. Biochemical parameters 15 days after treatment.

The results of the acute toxicity test reveal differences between the control group and the group exposed to the aqueous extract of *H. tuberculatum* (AEHT at 2000 mg/mL). However, it is crucial to stress that these variations were not statistically significant. ASAT levels were slightly higher in the AEHT group (360 IU/I) than in the control group (307.66 IU/I), and ALAT levels were also slightly higher in the AEHT group (46.82 IU/I) than in the control

group (43.46 IU/I). Similarly, urea levels were lower in the AEHT group (0.25 g/L) than in the control group (0.28 g/l). As for creatinine, there was a slight increase in the 2000mg/kg group compared with the control (-) group, with values of 3.8±0.36 and 3.56±0.40 mg/L, respectively. These variations, although observed, were not statistically significant. Although there were differences in liver and kidney parameters between the groups, the statistical non-significance underscores the need for further studies.

The results of acute HTAE toxicity revealed that body weights of mice increased significantly over the 15-day test period, with the exception of the 2000 mg/kg group, which showed a slight decrease between days 9 and 15. However, these differences were not statistically significant, indicating that *H. tuberculatum* extract has no effect on body weight.

Similarly, relative liver and kidney weights did not significantly differ between treatment and control groups, suggesting no effect of HTAE on organ weights. Biochemical analysis showed slight variations in liver and kidney parameters, but none were statistically significant, underlining that the toxicity of HTAE extract exceeds 2000 mg/kg. Overall, the aqueous extract of *H. tuberculatum* showed no significant toxicity in mice based on the parameters evaluated. The results obtained are in line with those reported in the study of Saidi et al. (2022). Within 24 hours of toxicological evaluation, aqueous and methanolic extracts induced behavioral changes, primarily altering sleep duration and causing mild anorexia compared to controls. No mortality occurred in any treatment group, suggesting an LD_{50} above 5g/kg, classifying *H. tuberculatum* aqueous and methanolic extracts as minimally toxic under the Global Harmonization System for Chemical Substances, category 5.

3.4. Hemolysis of rat red blood cells by HTAE

3.4.1. Evolution of HTAE absorbance in the hemolysis test

The hemolytic test performed on *H. tuberculatum* aims to assess its biocompatibility and potential harmlessness to blood cells. This *in vitro* assay examines the extract's substances to determine whether they can damage the membranes of erythrocytes, which release hemoglobin upon lysis. The evaluation was carried out on RCB exposed to different concentrations of HTAE, ranging from 39.06 to 625µg/mL. The results obtained (Figure 6) demonstrate a slight increase in absorbance levels observed at intervals of 0, 15, 30, and 60 minutes in a dose-dependent manner compared with the negative control. This result directly correlates with an escalation in the rate of hemolysis, indicating a proportional increase in hemolytic effect corresponding to higher extract concentrations.

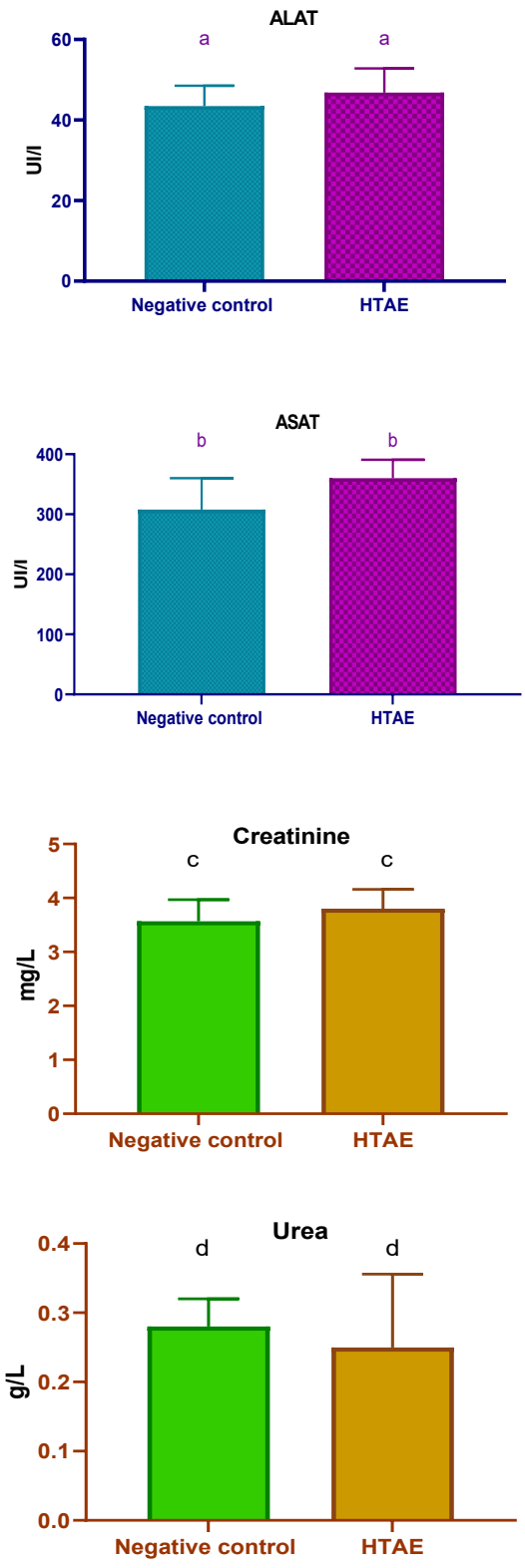

Figure 5. Effect of HTAE (2000 mg/kg) on biochemical parameters in treated animals. For each parameter, Bars with different letters represent statistically different values ($p < 0.05$)

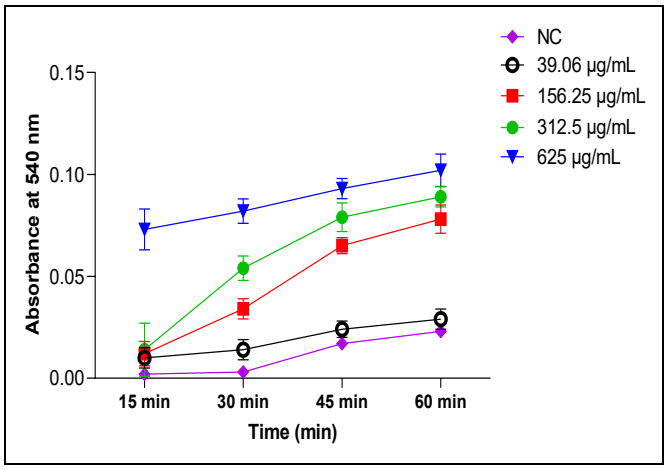

Figure 6. Evolution of absorbance at 540 nm of various concentrations of HTAE and negative control (NC) in the hemolysis test during 60 min.

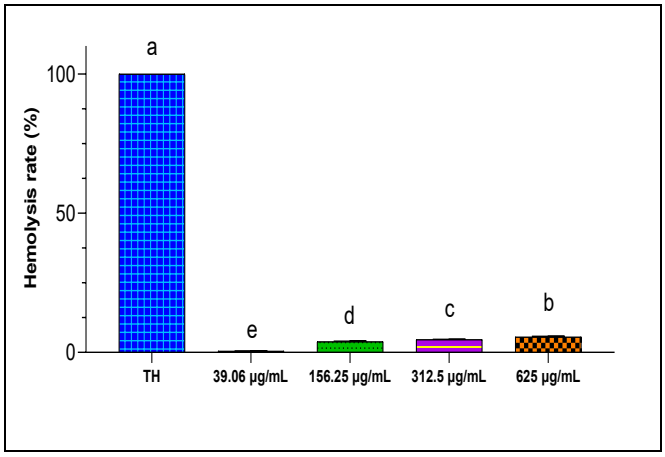

Figure 7. Hemolytic rate (%) of various concentrations of HTAE after 60 min of incubation compared to total hemolysis (TH). Bars with different letters represent statistically different values ($p < 0.05$).

In fact, the hemolysis test is a key indicator of cytotoxicity, measuring the degradation of rat RBC upon exposure to various concentrations of natural extracts. This evaluation serves as a pivotal method for assessing the cytotoxic effect of these extracts, making a significant contribution to the fields of phytotherapy and the formulation of pharmacological preparations. Generally, the hemolytic activity of a natural product or drug can occur through diverse mechanisms, ranging from cell membrane dissolution or increased permeability to complete cell lysis (Sayes et al., 2007). The observed low toxicity of the HTAE is attributed primarily to the presence of various phenolic compounds within the plant extract. In this context, previous reports suggest that the existence of phenolic compounds plays a substantial role in shielding the erythrocyte membrane against oxidation, thus imparting resistance against hemolytic activity (Ali et al., 2018). Eissa et al., (2013), reported that in the cellular model of oxidative stress using the human astrocytoma cell line U373-MG, pre-treatment with a concentration of 0.025 mg/mL of *H. tuberculatum* ethanolic extract significantly attenuated the loss of viability induced by H2O2, reducing it by 20.5%. In addition, the cytotoxic activity of the fractionated extracts of methanol (diethyl ether, chloroform, butanol, and water) was assessed on intact blood lymphocyte cells by the MTT (3-4,5-dimethylthiazol-2-yl)-2,5-diphenyltetrazolium bromide) assay. However, none of the fractionated extracts showed cytotoxicity against intact blood lymphocyte cells (Dastranj et al., 2019).

3.5. In silico study

Ankyrins are critical for maintaining the structural and functional integrity of red blood cells. Their role in linking the cell membrane to the cytoskeleton, stabilizing membrane proteins, and contributing to the overall shape and function of red blood cells is essential for their ability to transport oxygen and carbon dioxide efficiently throughout the body.

Docking of our phytochemicals into the active site of this protein showed remarkable affinity. Gallic Acid was the most active molecule with a glide gscore of -5.830 kcal/mol, followed by Rosmarinic acid with a glide gscore of -3.951 kcal/mol (Table 2).

Furthermore, the anion exchanger Band 3 in human erythrocytes is a multifunctional membrane protein that plays a central role in maintaining the cell's shape, regulating its pH, facilitating carbon dioxide transport, and ensuring proper ion balance. Its functions are essential for the overall health and functionality of red blood cells and, by extension, for oxygen transport and carbon dioxide removal throughout the body.

Rosmarinic acid was the molecule that showed the greatest affinity for the active site of the anion exchanger Band 3, with a glide score of -4.676 kcal/mol, followed by caffeic acid with a glide score of -4.279 kcal/mol (Table 2).

Hemoglobin, the oxygen-carrying protein found in red blood cells, plays an indirect but crucial role in maintaining the shape and structural integrity of red blood cells (erythrocytes). It also indirectly helps prevent hemolysis, which is the rupture or lysis of red blood cells. When red blood cells become too rigid or lose their characteristic biconcave shape, they can become more susceptible to mechanical stress and hemolysis. Hemoglobin's role in oxygen transport ensures that red blood cells maintain their flexibility and structural integrity, reducing the risk of hemolysis.

Rosmarinic acid and gallic Acid were the most active molecules in the active site of human hemoglobin with a glide score of -5.503 and -5.154 kcal/mol, respectively (Table 2).

Table 2. Results of ligands docking in active sites

	Glide g score		
	Human TRPV4 ankyrin (PDB : 4DX1)	Human erythrocyte Band 3 (PDB: 4YZF)	Human hemoglobin in the deoxy (PDB : 2DN2)
Caffeic Acid	-3.481	-4.279	-4.565
Gallic Acid	-5.83	-	-5.154
Rosmarinic acid	-3.951	-4.676	-5.503

The docking of gallic acid in the active site of the human TRPV4 ankyrin showed the formation of three hydrogen

bonds with residues GLN 317, and GLN 267 and one salt bridge with residue ARG 316 (Figure 8A and figure 9A).
Rosmarinic acid established a single hydrogen bond and a single salt bridge with the residue LYS 600 (Figure 8B and figure 9B).
In the active site of human hemoglobin, Rosmarinic acid has established five hydrogen bonds with residues THR C 38, LYS C 99, LYS A 99, and ASP A 94 and one Pi cation with residue LYS C 99, and one salt bridge with residue LYS A 99 (Figure 8C and figure 9C)

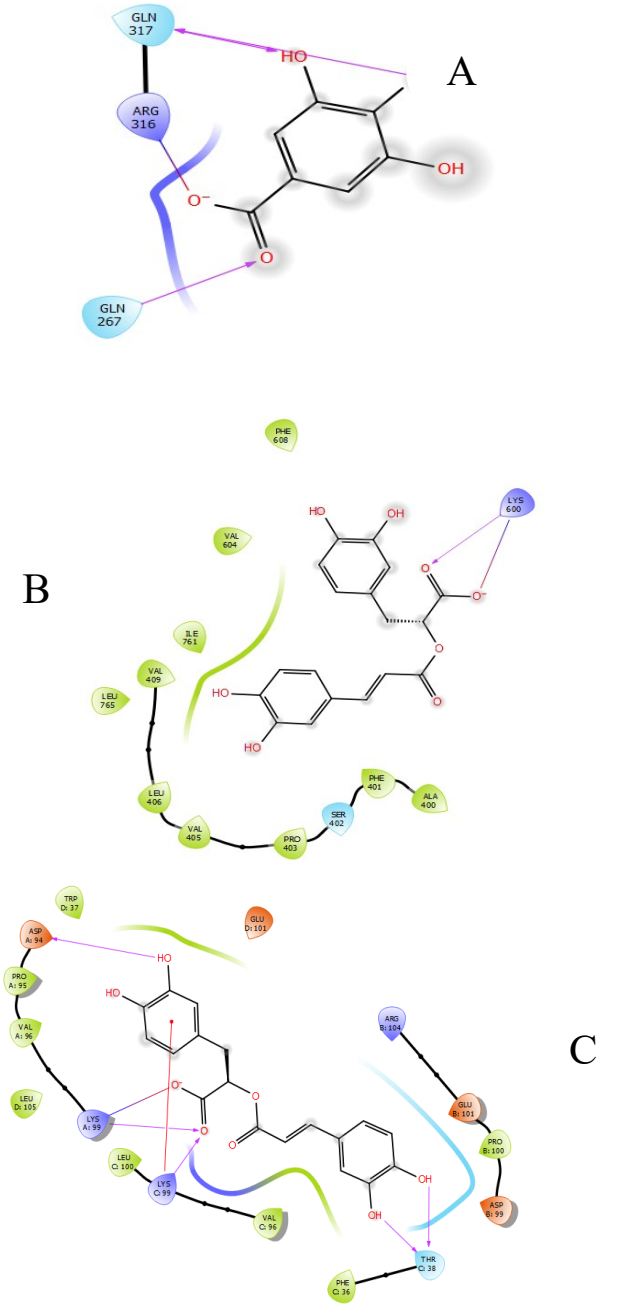

Figure 8. The 2D diagrams of the ligand's interactions with the active sites. A: gallic acid interactions with human TRPV4 ankyrin active site. B and C: Rosmarinic acid interactions with anion exchanger Band 3 and human hemoglobin active sites.

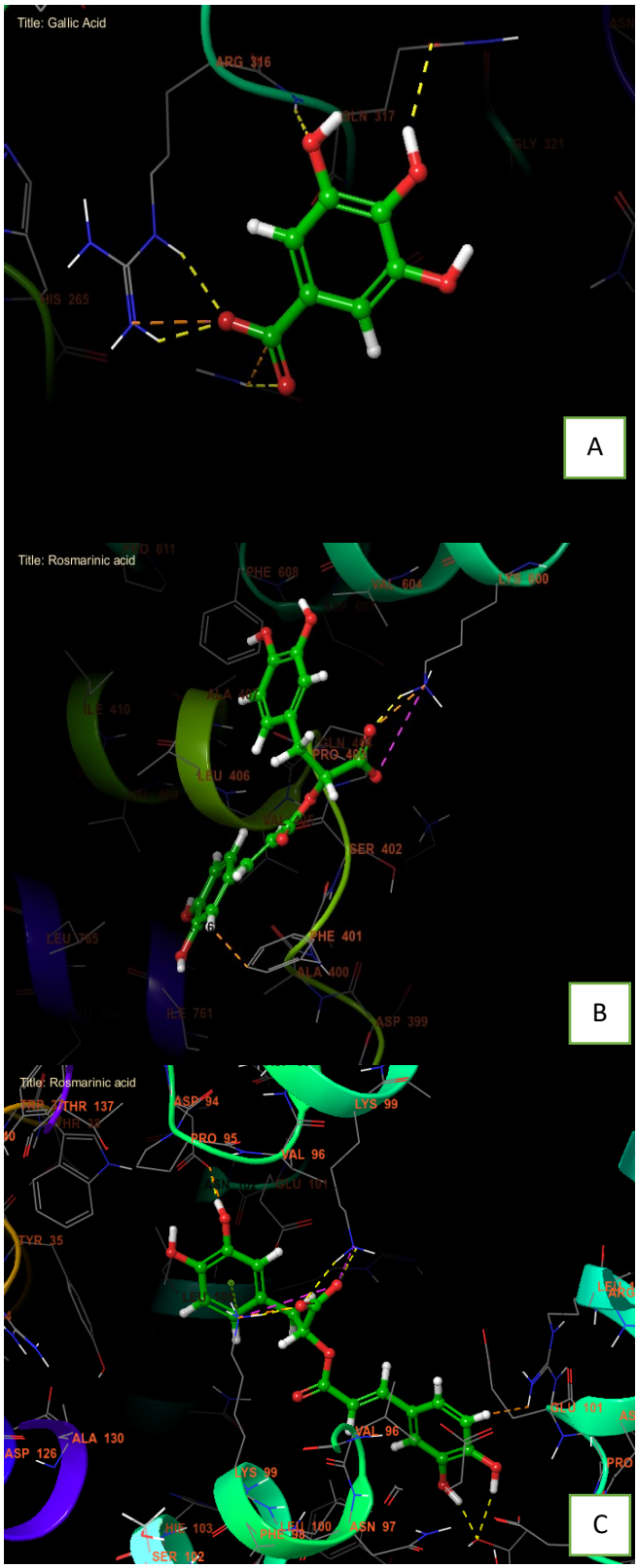

Figure 9. The 3D diagrams of the ligand's interactions with the active sites. A: gallic acid interactions with human TRPV4 ankyrin active site. B and C: Rosmarinic acid interactions with anion exchanger Band 3 and human hemoglobin active sites.

4. Conclusion

In this study, we report on the chemical composition of the aqueous extract of *H. tuberculatum*, its acute toxicity, and hemolytic activity. *H. tuberculatum* aqueous extract has high total polyphenol content. Body weight monitoring of animals treated at 1000 mg/kg and 2000 mg/kg for 14 days and measurement of relative organ weights and biochemical

parameters (ALAT, ASAT, urea, and creatinine) show that the *H. tuberculatum* aqueous extract is non-toxic, and that its LD_{50} exceeds the dose of 2000 mg/kg. The hemolytic effect against rat red blood cells was weak, suggesting the possibility of using *H. tuberculatum* aqueous extract orally with caution, since sub-acute and chronic toxicity tests must be carried out for long-term use of this extract.

Funding

This research received no external funding

Conflicts of Interest

The authors declare no conflicts of interest.

Data availability statement

Data will be available upon request from the corresponding author.

Ethical approval: Animals treated with the approval of the ethics committee of the faculty of sciences Dhar El Mahraz (LBEAS-February 2021)

References

Abdelkhalek, A., Salem, M.Z.M., Hafez, E., Behiry, S.I., 2020. the Antiviral Properties of Egyptian *Haplophyllum tuberculatum* Extract. Biology (Basel). 9, 1–17. https://doi.org/10.3390/biology9090248

Agour, A., Mssillou, I., El Barnossi, A., Chebaibi, M., Bari, A., Abudawood, M., Al-Sheikh, Y.A., Bourhia, M., Giesy, J.P., Aboul-Soud, M.A.M., Lyoussi, B., Derwich, E., 2023. Extracts of *Brocchia cinerea* (Delile) Vis Exhibit In Vivo Wound Healing, Anti-Inflammatory and Analgesic Activities, and Other In Vitro Therapeutic Effects. Life 13. https://doi.org/10.3390/life13030776

Al-Nour, M.Y., Arbab, A.H., Parvez, M.K., Mohamed, A.Y., Al-Dosari, M.S., 2021. In-vitro Cytotoxicity and In-silico Insights of the Multi-target Anticancer Candidates from *Haplophyllum tuberculatum*. Borneo J. Pharm. 4, 192–201. https://doi.org/10.33084/bjop.v4i3.1955

Al-Saeghi, S.S., Hossain, M.A., Al-Touby, S.S.J., 2022. Characterization of antioxidant and antibacterial compounds from aerial parts of *Haplophyllum tuberculatum*. J. Bioresour. Bioprod. 7, 52–62. https://doi.org/10.1016/j.jobab.2021.09.004

Ali, J., Irshad, R., Li, B., Tahir, K., Ahmad, A., Shakeel, M., Khan, N.U., Khan, Z.U.H., 2018. Synthesis and characterization of phytochemical fabricated zinc oxide nanoparticles with enhanced antibacterial and catalytic applications. J. Photochem. Photobiol. B Biol. 183, 349–356. https://doi.org/10.1016/j.jphotobiol.2018.05.006

AlQathama, A., Bader, A., Al-Rehaily, A., Gibbons, S., Prieto, J.M., 2022. In vitro cytotoxic activities of selected Saudi medicinal plants against human malignant melanoma cells (A375) and the isolation of their active principles. Eur. J. Integr. Med. 49, 102083.https://doi.org/10.1016/j.eujim.2021.102083

Amrati, F.E.-Z., Chebaibi, M., Galvao de Azevedo, R., Conte, R., Slighoua, M., Mssillou, I., Kiokias, S., de Freitas Gomes, A., Soares Pontes, G., Bousta, D., 2023a. Phenolic composition, wound healing, antinociceptive, and anticancer effects of *Caralluma europaea* extracts. Molecules 28, 1780. https://doi.org/10.3390/molecules28041780

Amrati, F.E.-Z., Slighoua, M., Mssillou, I., Chebaibi, M., Galvão de Azevedo, R., Boukhira, S., Moslova, K., Al Kamaly, O., Saleh, A., Correa de Oliveira, A., 2023b. Lipids Fraction from *Caralluma europaea* (Guss.): MicroTOF and HPLC Analyses and Exploration of Its Antioxidant, Cytotoxic, Anti-Inflammatory, and Wound Healing Effects. Separations 10, 172. https://doi.org/10.3390/separations10030172

Arabsalehi, F., Rahimmalek, M., Sabzalian, M.R., Ghanadian, M., Matkowski, A., Szumny, A., 2022. Changes in polyphenolic composition, physiological characteristics, and yield-related traits of Moshgak (*Ducrosia anethifolia* Boiss.) populations in response to drought stress. Protoplasma 1–19. DOI: 10.1007/s00709-022-01828-0

Bahorun, T., Gressier, B., Trotin, F., Brunet, C., Dine, T., Luyckx, M., Vasseur, J., Cazin, M., Cazin, J.C., Pinkas, M., 1996. Oxygen species scavenging activity of phenolic extracts from hawthorn fresh plant organs and pharmaceutical preparations. Arzneimittelforschung. 46, 1086–1089.

Boizot, N., Charpentier, J., Boizot, N., Méthode, J.C., 2020. Méthode rapide d ' évaluation du contenu en composés phénoliques des organes d ' un arbre forestier To cite this version : HAL Id : hal-02669118 Méthode rapide d ' évaluation du contenu en composés phénoliques des organes d ' un arbre forestier.

Bouslamti, M., Metouekel, A., Chelouati, T., El Moussaoui, A., Barnossi, A. El, Chebaibi, M., Nafidi, H.-A., Salamatullah, A.M., Alzahrani, A., Aboul-Soud, M.A.M., 2022. *Solanum elaeagnifolium* var. obtusifolium (Dunal) Dunal: Antioxidant, antibacterial, and antifungal activities of polyphenol-rich extracts chemically characterized by use of in vitro and in silico approaches. Molecules 27, 8688. https://doi.org/10.3390/molecules27248688

Dastranj, F., Karimi, F., Rahmani, N., 2019. Cytotoxic evaluations of metanolic extract fractions from *Haplophyllum tuberculatum* against RAJI and A549 cancerous cell lines. Iran. J. Biol. 31, 82–92. 20.1001.1.23832592.1397.31.1.9.5

Demma, J., Gebre-Mariam, T., Asres, K., Ergetie, W., Engidawork, E., 2007. Toxicological study on *Glinus lotoides*: a traditionally used taenicidal herb in Ethiopia. J. Ethnopharmacol. 111, 451–457. DOI: 10.1016/j.jep.2006.12.017

Djouahra Fahem, D., Bensmail, S., Bouteldja, R., Sara, M., Ferhoum, F., Bourfis, N., Acheuk, F., Fazouane, F., 2023. Characterization and antibacterial activity of alkaloids and polyphenols extracts from *Haplophyllum tuberculatum* (forssk.). Int. J. Second. Metab. 10, 495–510. https://doi.org/10.21448/ijsm.1248044

Eissa, T.F., González-Burgos, E., Carretero, M.E., Gómez-Serranillos, M.P., 2013. Biological activity of HPLC-characterized ethanol extract from the aerial parts of *Haplophyllum tuberculatum*. Pharm. Biol. 52, 151–156. 10.3109/13880209.2013.819517

El Abdali, Y., Mahraz, A.M., Beniaich, G., Mssillou, I.,

Chebaibi, M., Bin Jardan, Y.A., Lahkimi, A., Nafidi, H.-A., Aboul-Soud, M.A.M., Bourhia, M., 2023. Essential oils of *Origanum compactum* Benth: Chemical characterization, in vitro, in silico, antioxidant, and antibacterial activities. Open Chem. 21, 20220282. doi.org/10.1515/chem-2022-0282

Fofana, F.G., Ksouri, A., Cisse, C., Souiai, O., Benkahla, A., Sangare, M., Shaffer, J.G., Doumbia, S.O., Wele, M., n.d. Docking of Human Band 3 Anion Transporter Proteins with Their Plasmodium Falciparum Interactors Based on Short Linear Motifs. Available SSRN 4053257.

Khalid, S.A., Waterman, P.G., 1981. Alkaloid, lignan and flavonoid constituents of *Haplophyllum tuberculatum* from Sudan. Planta Med. 43, 148–152. 10.1055/s-2007-971491

Gharibi, S., Sayed Tabatabaei, B.E., Saeidi, G., Talebi, M., Matkowski, A., 2019. The effect of drought stress on polyphenolic compounds and expression of flavonoid biosynthesis related genes in *Achillea pachycephala* Rech.f. Phytochemistry 162, 90–98. https://doi.org/10.1016/j.phytochem.2019.03.004

Hadjadj, S., Bayoussef, Z., El Hadj-Khelil, A.O., Beggat, H., Bouhafs, Z., Boukaka, Y., Khaldi, I.A., Mimouni, S., Sayah, F., Tey, M., 2015. Ethnobotanical study and phytochemical screening of six medicinal plants used in traditional medicine in the Northeastern Sahara of Algeria (area of Ouargla). J Med Plants Res 9, 1049–1059. DOI: 10.5897/ JMPR2015.5932

Hamdi, A., Majouli, K., Abdelhamid, A., Marzouk, B., Belghith, H., Chraief, I., Bouraoui, A., Marzouk, Z., Heyden, Y. Vander, 2018a. Pharmacological activities of the organic extracts and fatty acid composition of the petroleum ether extract from *Haplophyllum tuberculatum* leaves. J. Ethnopharmacol. 216, 97–103. https://doi.org/10.1016/j.jep.2018.01.012

Hamdi, A., Viane, J., Mahjoub, M.A., Majouli, K., Gad, M.H.H., Kharbach, M., Demeyer, K., Marzouk, Z., Heyden, Y. Vander, 2018b. Polyphenolic contents, antioxidant activities and UPLC–ESI–MS analysis of *Haplophyllum tuberculatum* A. Juss leaves extracts. Int. J. Biol. Macromol. 106, 1071–1079. https://doi.org/10.1016/j.ijbiomac.2017.08.107

Joslyn, M.A., 1970. A serie of monographies. J. Food Sci. Technol. 2ème Ed. B.

Junior, C.M.S., Silva, S.M.C., Sales, E.M., da Silva Velozo, E., Dos Santos, E.K.P., Canuto, G.A.B., Azeredo, F.J., Barros, T.F., Biegelmeyer, R., 2023. Coumarins from Rutaceae: Chemical diversity and biological activities. Fitoterapia 168, 105489. https://doi.org/10.1016/j.fitote.2023.105489

Kifayatullah, M., Mustafa, M.S., Sengupta, P., Sarker, M.M.R., Das, A., Das, S.K., 2015. Evaluation of the acute and sub-acute toxicity of the ethanolic extract of *Pericampylus glaucus* (Lam.) Merr. in BALB/c mice. J. Acute Dis. 4, 309–315.

Lafraxo, S., El Moussaoui, A., A Bin Jardan, Y., El Barnossi, A., Chebaibi, M., Baammi, S., Ait Akka, A., Chebbac, K., Akhazzane, M., Chelouati, T., 2022. GC-MS Profiling, In Vitro Antioxidant, Antimicrobial, and In Silico NADPH Oxidase Inhibition Studies of Essential Oil of *Juniperus thurifera* Bark. Evidence-Based Complement. Altern. Med. 2022, 6305672. DOI: 10.1155/2022/6305672

Mahmoud, A.B., Danton, O., Kaiser, M., Han, S., Moreno, A., Algaffar, S.A., Khalid, S., Oh, W.K., Hamburger, M., Mäser, P., 2020a. Lignans, amides, and saponins from *haplophyllum tuberculatum* and their antiprotozoal activity. Molecules 25, 3–15. https://doi.org/10.3390/molecules25122825

Mahmoud, A.B., Mäser, P., Kaiser, M., Hamburger, M., Khalid, S., 2020b. Mining sudanese medicinal plants for antiprotozoal agents. Front. Pharmacol. 11, 543689. https://doi.org/10.3389/fphar.2020.00865

Mirniyam, G., Rahimmalek, M., Arzani, A., Matkowski, A., Gharibi, S., Szumny, A., 2022. Changes in Essential Oil Composition, Polyphenolic Compounds and Antioxidant Capacity of Ajowan (*Trachyspermum ammi* L.) Populations in Response to Water Deficit. Foods 11. https://doi.org/10.3390/foods11193084

Mohamed Mohamed Sabry, O., Mohamed El Sayed, A., Khalid Alshalmani, S., 2016. GC/MS Analysis and Potential Cytotoxic Activity of *Haplophyllum tuberculatum* Essential Oils Against Lung and Liver Cancer Cells. Pharmacogn. J. 8, 66–69.

Mohammadhosseini, M., Venditti, A., Frezza, C., Serafini, M., Bianco, A., Mahdavi, B., 2021. The genus haplophyllum juss.: Phytochemistry and bioactivities—A review, Molecules. https://doi.org/10.3390/molecules26154664

Mssillou, I., Agour, A., Lyoussi, B., Derwich, E., 2021. Chemical Constituents, In Vitro Antibacterial Properties and Antioxidant Activity of Essential Oils from *Marrubium vulgare* L. Leaves.Trop. J. Nat. Prod. Res. 5, 661–667. doi. org/10.26538/tjnpr/v5i4. 12

Mssillou, I., Agour, A., Slighoua, M., Chebaibi, M., Amrati, F.E.Z., Alshawwa, S.Z., Al Kamaly, O., El Moussaoui, A., Lyoussi, B., Derwich, E., 2022. Ointment-Based Combination of *Dittrichia viscosa* L. and *Marrubium vulgare* L. Accelerate Burn Wound Healing. Pharmaceuticals 15, 1–13. https://doi.org/10.3390/ph15030289

Nair, R., Shukla, V., Chanda, S., 2009. Effect of single dose administration of *Polyalthia longifolia* (Sonn.) Thw. var. pendula leaf on gross behavioral assessment in mice. Indian Drugs 46, 116–123.

Ouahabi, S., Loukili, E.H., Daoudi, N.E., Chebaibi, M., Ramdani, M., Rahhou, I., Bnouham, M., Fauconnier, M.-L., Hammouti, B., Rhazi, L., 2023. Study of the phytochemical composition, antioxidant properties, and in vitro anti-diabetic efficacy of *Gracilaria bursa-pastoris* extracts. Mar. Drugs 21, 372. https://doi.org/10.3390/md21070372

Ramadan, A., Soliman, G., Mahmoud, S.S., Nofal, S.M., Abdel-Rahman, R.F., 2012. Evaluation of the safety and antioxidant activities of *Crocus sativus* and Propolis ethanolic extracts. J. Saudi Chem. Soc. 16, 13–21. https://doi.org/10.1016/j.jscs.2010.10.012

Saidi, A., Hambaba, L., Bensaad, M.S., Melakhessou, M.A., Bensouici, C., Ferhat, N., Kahoul, M.A., Helal, M., Sami, R., 2022. Phenolic Characterization

Using cLC-DAD Analysis and Evaluation of In Vitro and In Vivo Pharmacological Activities of *Ruta tuberculata* Forssk. https://doi.org/10.3390/antiox11071351

Saleh, E.A.M., Khan, A.U., Tahir, K., Almehmadi, S.J., Al-Abdulkarim, H.A., Alqarni, S., Muhammad, N., Dawsari, A.M.A.L., Nazir, S., Ullah, A., 2021. Phytoassisted synthesis and characterization of palladium nanoparticles (PdNPs); with enhanced antibacterial, antioxidant and hemolytic activities. Photodiagnosis Photodyn. Ther. 36, 102542. https://doi.org/10.1016/j.pdpdt.2021.102542

Sayes, C.M., Reed, K.L., Warheit, D.B., 2007. Assessing toxicity of fine and nanoparticles: comparing in vitro measurements to in vivo pulmonary toxicity profiles. Toxicol. Sci. 97, 163–180. DOI: 10.1093/toxsci/kfm018

Tellone, E., Ficarra, S., Russo, A., Bellocco, E., Barreca, D., Laganà, G., Leuzzi, U., Pirolli, D., De Rosa, M.C., Giardina, B., 2012. Caffeine inhibits erythrocyte membrane derangement by antioxidant activity and by blocking caspase 3 activation. Biochimie 94, 393–402. DOI: 10.1016/j.biochi.2011.08.007

Varamini, P., Doroudchi, M., Mohagheghzadeh, A., Soltani, M., Ghaderi, A., 2007. Cytotoxic evaluation of four Haplophyllum species with various tumor cell lines. Pharm. Biol. 45, 299–302. https://doi.org/10.1080/13880200701214938

Wu, Z., Chen, L., 2022. Similarity-Based Method with Multiple-Feature Sampling for Predicting Drug Side Effects. Comput. Math. Methods Med. 2022. https://doi.org/10.1155/2022/9547317

Zhou, T., Wang, Z., Guo, M., Zhang, K., Geng, L., Mao, A., Yang, Y., Yu, F., 2020. Puerarin induces mouse mesenteric vasodilation and ameliorates hypertension involving endothelial TRPV4 channels. Food Funct. 11, 10137–10148.DOI: 10.1039/d0fo02356f